

Chapter 3

Expression of $\alpha 5$ -mEGFP in Mouse Cortical Neurons

Subcellular localization of the neuronal nAChR subtypes $\alpha 4\beta 2$ and $\alpha 4\beta 4$ depends on the β subunit. Signal sequences in the M3-M4 loop of β nAChRs bind protein factors to enable or inhibit forward trafficking for expression on the cell membrane. The M3-M4 loops of some subunits, like $\beta 4$, contain forward trafficking signals that contribute to the abundant expression of receptors containing those subunits at the cell surface [35]. However, many subtypes, such as those that contain the $\beta 2$ subunit, are primarily retained in the ER. For these receptors, molecular chaperones such as nicotine may aid in surface expression [23, 36]. The presence of these intracellular trafficking sequences may act as an intra-receptor level of nAChR regulation. The $\alpha 4\beta 2$ receptor can exist in two stoichiometries, one of which traffics more readily to the membrane [23]. This difference in trafficking between stoichiometries may be partially due to the number of beta subunits contained in the receptor. An RRQR retention motif has been identified in the M3-M4 loop of the nAChR $\beta 2$ subunit. The $(\alpha 4)_3(\beta 2)_2$ receptor traffics to the membrane more easily than $(\alpha 4)_2(\beta 2)_3$ because the $(\alpha 4)_2(\beta 2)_3$ stoichiometry contains more beta subunits and therefore more RRQR signals [23, 37]. nAChRs may also use incorporation of accessory subunits such as $\alpha 5$ and $\beta 3$ to modulate trafficking and expression.

Examination of the $\alpha 5$ M3-M4 loop identified a forward trafficking IFL amino acid motif beginning at position 354 and a LCM motif at position 364. I/LXM motifs, where X can be any amino acid, have been associated with vesicular export from the endoplasmic reticulum. The I/LXM sequence interacts with a surface groove of Sec24D, a major component of COPII vesicles, for efficient cargo packaging [38]. Presence of Sec24D

targeting sequences in the $\alpha 5$ subunit imply that incorporation of an $\alpha 5$ into a parent receptor may encourage trafficking of the $\alpha 5^*$ receptor to the plasma membrane via interaction with Sec24D and other COPII machinery. When $\alpha 5$ is incorporated into an $\alpha 4\beta 2$ receptor, the receptor stoichiometry becomes fixed as $\alpha 5(\alpha 4\beta 2)_2$. This $\alpha 5(\alpha 4\beta 2)_2$ receptor contains two ER retention RRQR signals from the $\beta 2$ subunits and one IFL motif in the M3-M4 loop of the $\alpha 5$ subunit. We hypothesized that due to the reduction in retention sequences and the addition of a forward trafficking signal $\alpha 5\alpha 4\beta 2$ receptors may be more easily expressed on the cell membrane than $\alpha 4\beta 2$ receptors.

To assay whether $\alpha 5\alpha 4\beta 2$ receptors are trafficked differently than $\alpha 4\beta 2$ receptors, we first expressed these receptors heterologously in clonal cell lines N2a and HEK293. Cells were imaged live, 48 h post-transfection, at 37 °C with a Nikon C1 scanning confocal microscope. In all fluorescence experiments the percentage of cells with detectable $\alpha 5$ -mEGFP fluorescence is low when compared to $\alpha 4$ -mEGFP and $\beta 3$ -mYFP controls. Even after optimization of transfection, expression, and imaging protocols, $\alpha 5$ -mEGFP fluorescence remained $\leq 50\%$ of control subunit levels. It is possible that like $\alpha 7^*$ receptors, whose expression is significantly enhanced by co-expression with the chaperone protein Ric-3, $\alpha 5^*$ receptors rely on endogenous protein chaperones or other factors for optimal expression, and $\alpha 5$ -mEGFP may be more efficiently expressed in primary cells [39]. To test this hypothesis, $\alpha 5$ -mEGFP was expressed in primary cultures of mouse neurons.

$\alpha 5$ -mEGFP plasmid DNA was transiently transfected into mouse cortical neurons alongside unlabeled $\alpha 4$ and $\beta 2$ subunits. Due to the difficulty of imaging primary neurons, cells expressing nAChRs were fixed with 4% paraformaldehyde (PFA) before

imaging. 48 h post-transfection cells were fixed, washed with 1% phosphate buffered saline (PBS), and imaged in PBS at room temperature after excitation with a 488nm laser. Images were spectrally unmixed against control spectra for mEGFP and background controls. When transfected with only $\alpha 4$ -mEGFP and $\beta 2$ plasmid DNA, mouse e17 cortical neurons express $\alpha 4$ -mEGFP $\beta 2$ with a transfection efficiency of approximately 10% (figure 3.1). When $\alpha 5$ -mEGFP is transfected with unlabeled $\alpha 4$ and $\beta 2$ subunits, very low intensity of $\alpha 5$ -mEGFP fluorescence is seen. In addition to reduced fluorescence, a cell death rate of over 50% is observed. Unlike $\alpha 4$ -mEGFP, $\alpha 5$ -mEGFP exhibits low intensity fluorescence that is confined to the cell bodies (see figure 3.1B). Interestingly, when a red fluorescent $\alpha 4$ -mCherry is transfected with green fluorescent $\alpha 5$ -mEGFP and unlabeled $\beta 2$, all detected fluorescence, not just that from $\alpha 5$ -mEGFP, is confined to the cell body (figure 3.1D). This is not true when fluorescent $\alpha 4$ subunits are transfected with unlabeled $\beta 2$ subunits alone (figure 3.1C).

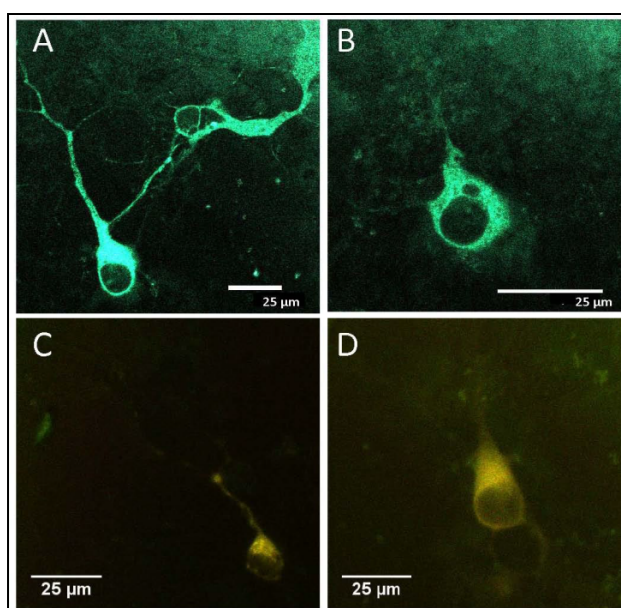


Figure 3.1

Mouse e17 cortical neurons expressing fluorescent nAChRs. Cells were transfected after 6 days in culture, fixed with 4% PFA and imaged 48 h post transfection. Samples were exposed to 488 nm (mEGFP) or 561 nm (mCherry) laser excitation and spectrally unmixed against control spectra for mEGFP and mCherry.

Scale = 25 microns

A) $\alpha 4$ -mEGFP $\beta 2$ – fluorescence is fairly bright and extends into the processes. Laser intensity = 15%.

B) $\alpha 5$ -mEGFP $\alpha 4\beta 2$ – fluorescence is dim and restricted to the cell body. Laser intensity = 35%

C) $\alpha 4$ -mEGFP $\alpha 4$ -mCherry $\beta 2$ – overlay of images obtained using 488nm and 561 nm excitation. Laser intensity = 15%.

D) $\alpha 5$ -mEGFP $\alpha 4$ -mCherry $\beta 2$ – overlay of images obtained using 488 nm and 561 nm excitation. Laser intensity = 35% and 15%, respectively.

We see that fluorescence from $\alpha 4$ -mEGFP is distributed into the neuronal processes, but when the $\alpha 5$ subunit is present, fluorescence is restricted to the cell body. It is possible that insertion of a fluorophore disrupted the efficiency of expression of $\alpha 5$ -mEGFP. However, It is interesting to note that it is not the presence of the mEGFP in the intracellular loop that contributes to the expression problem. $\alpha 5$ -mEGFP subunits constructed such that the mEGFP has been fused to the extracellular C-terminal domain of the $\alpha 5$ subunit, leaving the M3-M4 loop clear of any manipulation were also transiently transfected into mouse cortical neurons with the same lack of success.

Given the high rate of cell death, attempts were made to optimize the neuronal transfection protocol. It was found that transfecting neurons in a lower volume of growth media (0.5 mL), combined with complete replacement of cellular medium following 4 h 37 °C incubation with the lipofection-DNA complex, greatly enhanced both transfection efficiency and cell viability (see appendix ii for complete optimized protocol). This optimization has eliminated the need for fixed cell imaging techniques. Using the CO₂ buffering Leibovitz media in the absence of phenol red, a small 37 °C incubator installed on the microscope stage, and a heating unit that warms the objective itself to 37 °C, it is possible to maintain live cell health during an imaging session for upwards of 1 h before apoptotic phenotypes are observed.

Figure 3.2A shows the poor expression and low fluorescence previously seen in the fixed neurons transiently transfected with $\alpha 5$ -mGFP $\alpha 4$ $\beta 2$ receptor subunits. The multiple cells in the single imaging field shown in figure 1C illustrate the improvements to the transfection efficiency over those previously used, and increased expression and visualization of the $\alpha 5$ -mEGFP subunit after optimization of culture, transfection, and

imaging conditions. It is also important to note the increased fluorescence intensity and the improved distribution of fluorescence of the cells in shown in figure 3.2B and 3.2D when compared to the fixed cell shown in 3.2A. Improved transfection and cell culturing methods have allowed us to visualize more than just the cell soma. Figures 3.2B and 3.2D show that $\alpha 5$ -mEGFP expression in live neuronal culture extends from the soma into both primary and secondary processes of the neuron.

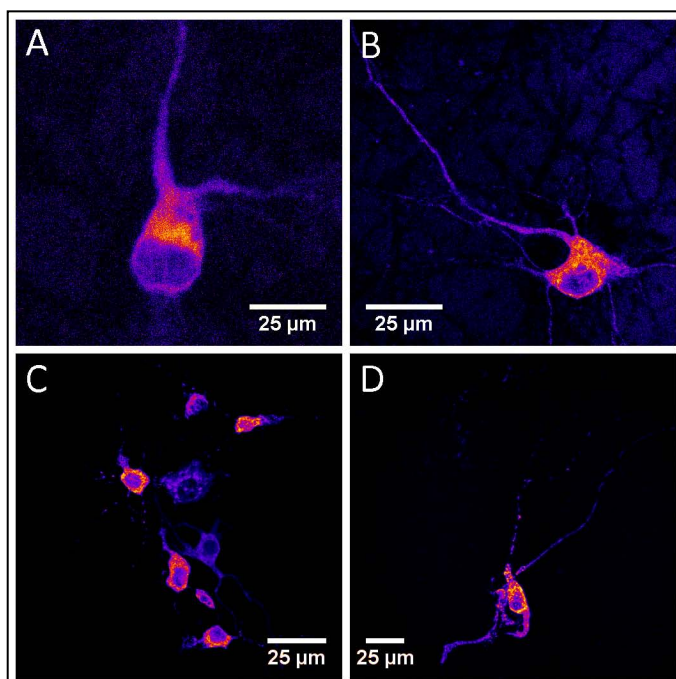


Figure 3.2

Mouse e17 cortical neurons expressing $\alpha 5$ -mEGFP. Cells were transfected after 6 d in culture and imaged 24 h post-transfection. All images were taken with a scanning confocal microscope after excitation with 488 nm laser.

A. Expression of $\alpha 5$ -mEGFP $\alpha 4\beta 2$ using non-optimized transfection protocol. Image was taken after fixation with 4% PFA, 24 h post-transfection.

B and D. Expression of $\alpha 5$ -mEGFP $\alpha 4\beta 2$ under optimized cell culture and transfection protocol. Cells were imaged live, without fixation, 48 h post-transfection.

C. Widefield image of multiple fluorescent neurons in a dish illustrates the significant improvements in transfection achieved using the optimized protocol.

We know from previous experiments performed in HEK293 and N2a cells that $\alpha 5$ -mEGFP or $\alpha 5D398N$ -mEGFP subunits co-localize with $\alpha 4$ and $\beta 2$ receptor subunits (chapter 4). $\alpha 5$ -mEGFP or $\alpha 5D398N$ -mEGFP subunits also form functional receptors with $\alpha 4$ and $\beta 2$ receptor subunits in frog oocytes (chapter 1). The improvements made to experimental techniques have allowed us to ask whether $\alpha 5$ -mEGFP or $\alpha 5D398N$ -mEGFP subunits co-localize with $\alpha 4$ and $\beta 2$ receptor subunits in primary cell cultures. Figure 3.3 shows example images of co-transfection experiments with $\alpha 5$ -mEGFP or $\alpha 5D398N$ -mEGFP, $\alpha 4$ -

mCherry, and unlabeled $\beta 2$ subunits. This is the first reported expression of a mutant $\alpha 5 D 3 9 8 N$ -mEGFP subunit in mouse neurons.

As stated in the introduction, the SNP rs16969968 encodes a D to N substitution in the M3-M4 loop of the $\alpha 5$ subunit at position 398 and is associated with increased risk for nicotine dependence in humans [18]. It was hypothesized that the M3-M4 loop localization of the D398N mutation may contribute to changes in intracellular trafficking or localization of the mutant protein. Co-transfection experiments did not reveal any differences in localization between $\alpha 4$ -mCherry and expressed $\alpha 5$ -mEGFP and $\alpha 5 D 3 9 8 N$ -mEGFP subunits (figure 3.3). This could indicate proper expression and assembly of $\alpha 5$ -mGFP, $\alpha 4$ -mCherry, and $\beta 2$ into $\alpha 5$ -mGFP $\alpha 4$ -mCherry $\beta 2$ receptors; unfortunately, no obvious differences in expression were seen upon introduction of the $\alpha 5 D 3 9 8 N$ -mEGFP subunit.

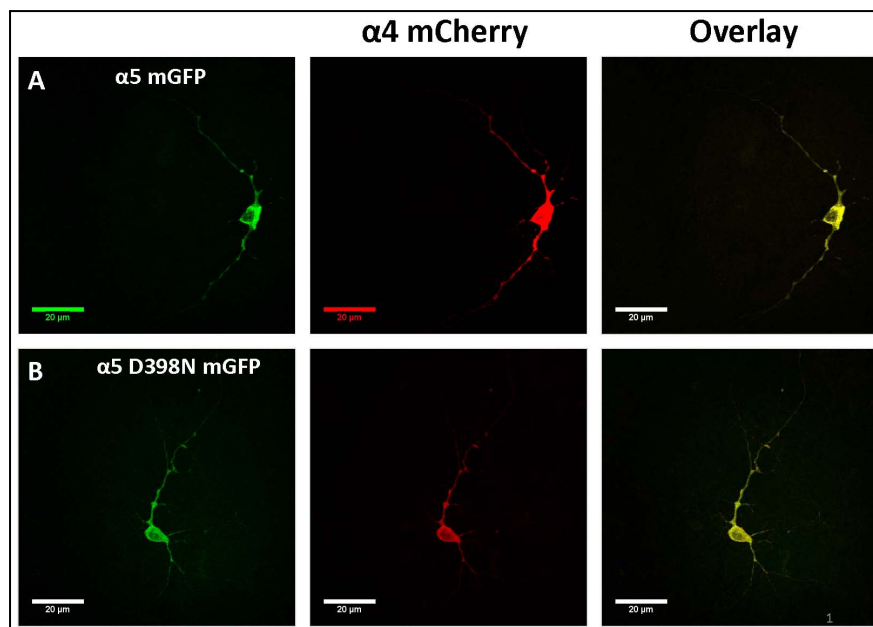
Figure 3.3

A. False color images (left to right) of $\alpha 5$ -mEGFP $\alpha 4$ -mCherry, and an overlay of the $\alpha 5$ -mEGFP $\alpha 4$ -mCherry images.

B. False color images (left to right) of $\alpha 5 D 3 9 8 N$ -mEGFP $\alpha 4$ -mCherry, and an overlay of the $\alpha 5$ -mEGFP $\alpha 4$ -mCherry images.

All images are max-intensity projections of 1 micron step size z-stacks. Imaging was performed with a scanning confocal microscope after sample excitation by 488 nm for the mEGFP (green) or 561 nm for mCherry (red).

All scale bars 20 microns.



Co-localization studies performed on cells expressing $\alpha 5$ -mEGFP, $\alpha 4$, $\beta 2$, and the ER marker dsRed-ER show a 1:1 correlation with ER marker and localization of $\alpha 5$ -mEGFP (figure 3.4). Chronic or acute incubation with nicotine may rescue ER localization of $\alpha 5$ -mEGFP and facilitate ER exit of $\alpha 5$ -mEGFP containing receptors, possibly through a chaperoning-like mechanism. 4 h treatment of neurons transiently transfected with $\alpha 5$ -mEGFP, $\alpha 4$, $\beta 2$, and dsRed-ER with 1.0 μ M nicotine did not result in measurable changes in localization with ER marker. Other concentrations of nicotine were also investigated but no changes were observed.

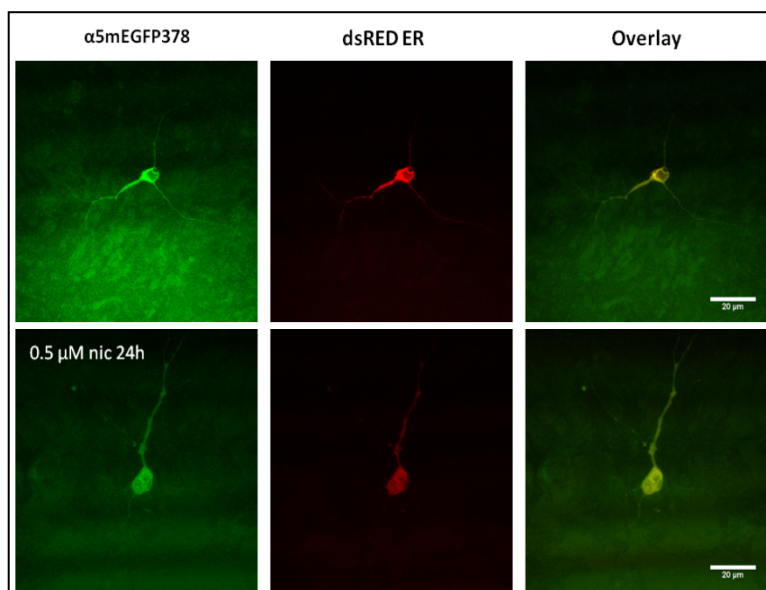


Figure 3.4

Representative images of mouse e17 cortical neurons expressing $\alpha 5$ -mEGFP subunits with non-fluorescent $\alpha 4$ and $\beta 2$ subunits. Neurons were concurrently transfected with dsRED-ER, to delineate the endoplasmic reticulum.

Fluorescent expression of $\alpha 5$ -mEGFP was characteristically low, and no obvious differences in co-localization with dsRED-ER were seen after 24 h incubation with 0.5 μ M nicotine.

24 h incubations were performed with 0.1 μ M nicotine, and the same result was seen. Parallel experiments conducted with the $\alpha 5D398N$ -mEGFP mutant variant were performed for both 4 h and 24 h incubations, and no difference in co-localization with ER marker or phenotypic differences between $\alpha 5$ -mEGFP and $\alpha 5D398N$ -mEGFP were observed (figure 3.5).

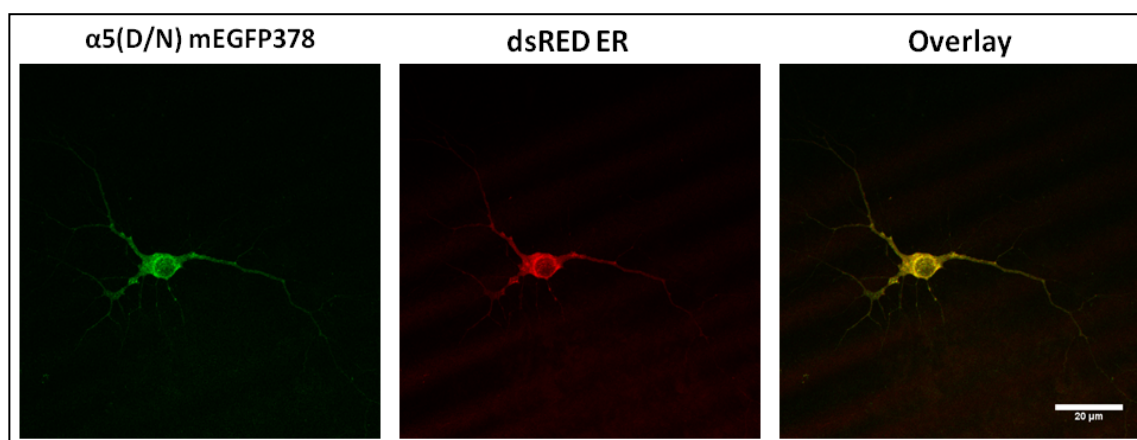


Figure 3.5

Representative images of $\alpha 5D398N$ -mEGFP and ER marker dsRED-ER. Images were taken by scanning confocal microscope after excitation with 488 nm (mEGFP) or 561 nm (dsRED-ER) laser. Scale = 20 μ m. mEGFP images perfectly overlay with dsRED ER images, indicating that there is little expression of $\alpha 5D398N$ -mEGFP outside the ER.

It is possible that differences in trafficking do occur, but the effects are subtle. Measurements of integrated membrane expression using Total Internal Reflection Fluorescence (TIRF) have been used to quantify differences in surface expression of $\alpha 4\beta 2$ receptors after drug exposures [23]. Similar techniques could be applied to neurons expressing $\alpha 4$ vs $\alpha 5$ and/or $\alpha 5D/N$ subunits. With the data reported here we are able to demonstrate expression of fluorescent $\alpha 5$ -mEGFP and $\alpha 5D/N$ -mEGFP constructs in mouse e17 cortical neurons. Optimized protocols for transfection, expression and imaging of these neurons are described in detail in appendix ii. Similar to results reported in chapter 1, even after optimization of imaging conditions, expression of fluorescent $\alpha 5$ is consistently low compared to other fluorescent α subunits. If we wish to study the endogenous behaviors of $\alpha 5^*$ receptors, it is possible that other methods for fluorescent labeling must be used to improve visualization and ensure wild-type behavior of the labeled receptor.

From these data, we must conclude that there is little difference in trafficking of $\alpha 4$ -mEGFP $\beta 2$ vs. $\alpha 5$ -mEGFP $\alpha 4\beta 2$ receptors. $\alpha 5$ -mEGFP $\alpha 4\beta 2$ receptors express much less efficiently, and $\alpha 5$ -mEGFP fluorescence does not extend as far into the neuronal processes

as does $\alpha 4$ -mEGFP, but this is most likely due to the large difference in expression level and not the result of differential trafficking. Incubation with $1\mu\text{M}$ nicotine was not able to rescue ER localization of either the $\alpha 5$ mEGFP $\alpha 4\beta 2$ or $\alpha 5\text{D}$ /NmEGFP $\alpha 4\beta 2$ receptor and no difference in expression or subcellular localization of these two receptors was seen. Taken together, these data suggest that the D398N mutation does not exert its influence over $\alpha 5$ mEGFP $\alpha 4\beta 2$ by altering assembly or trafficking of the receptor.